SPICAM and SPICAV data level 1B IR
Process description

Version	Date	Comments
1	19/12/2014	
2	09/07/2015	
3	28/10/2025	Add section 4.5.2 Correcting long term trend in SPICAM IR

Prepared by:	Approved by:
NICOLAS CHAPRON (Version 1,2) **SVETLANA GUSLYAKOVA (Version 1,2)** **LOIC VERDIER (version 3)**	**ANNA FEDOROVA (Version 1,2)**

1 Introduction 2
1.1 Purpose 2
1.2 Reference documents 2
1.3 Abbreviations 2
2 Overall overview of the process 3
3 Pre-processing 3
3.1 FITS formatting 3
3.2 Missing data processing 3
4 Correction process description 3
4.1 Data overlapping correction 4
4.2 Dark Current correction 5
4.3 Wavelength calibration 7
4.4 Correlation of geometry and data points 8
4.5 Radiometric calibration 9

1 Introduction

1.1 Purpose

This document provides a description for the different process applied on the raw SPICAM and SPICAV IR data to obtain the level 1B. Concatenated with the geometry, the data in the level 1B is corrected from the missing packets, the dark current, the RF-wavelength c and absolute radiometric calibration is applied. The algorithm of wavelength-geometry correlation is also presented. The 1B level is available only for N, L and E (O_2 nightglow command) measurements.

1.2 Reference documents

Ref N°	Title	Author	Date
1	otchet_express_vex_mars2013_v8.doc	Anna Fedorova	19/12/2011
2	SPICAM IR acousto-optic spectrometer experiment on Mars Express	Korablev et al.	J. Geophys. Res. 111 (E9), 2006
3	Exploration of Mars in SPICAM-IR experiment onboard the Mars-Express spacecraft: 1. Acousto-optic spectrometer SPICAM-IR	Korablev et al.	Cos. Res. 44 (4), 278-293 2006
4	SPICAV IR acousto-optic spectrometer experiment on Venus Express	Korablev et al.	Planet. Space Sci. 65 (1), 38-57

1.3 Abbreviations

ADC	Analog-to-digital converter
ADU	Analog to Digital Unit
AOTF	Acousto-optical tunable filter
DC	Dark Current
DDS	Data Distribution System
FITS	Flexible Image Transport System
FWHM	Full Width at Half Maximum
IR	Infrared
LW	Long Wavelength Channel
MEx	Mars-Express
NaN	Not a Number
RF	Radio frequency
SPICAM	Spectroscopy for Investigation of Characteristics of the Atmosphere of Mars
SPICAV	Spectroscopy for Investigation of Characteristics of the Atmosphere of Venus
SW	Short Wavelength Channel
VEx	Venus-Express

2 Overall overview of the process

The following diagram represents an overall overview of the correction process:

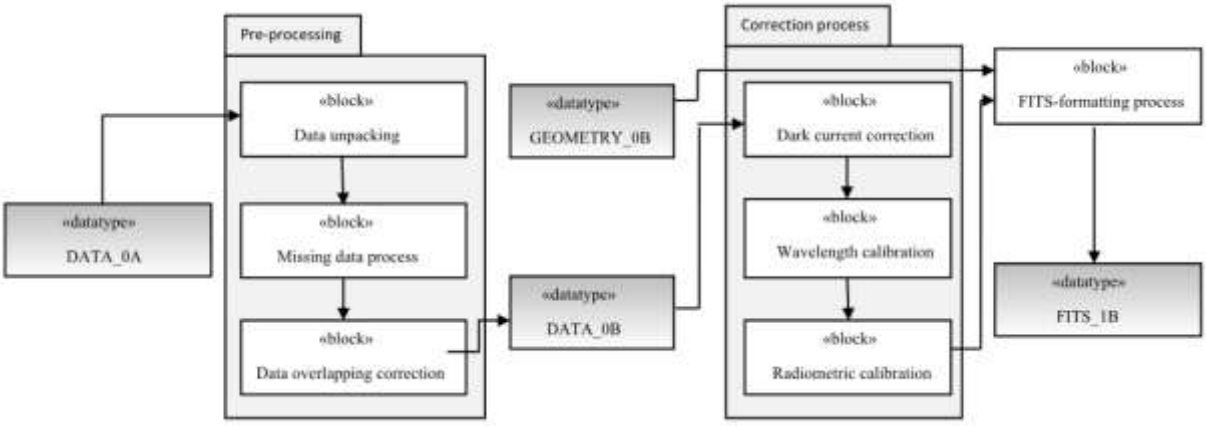

3 Pre-processing

3.1 FITS formatting

In the level 0B (raw), the data and geometry are available in two different files. For convenient use, both data and geometry are concatenated in one file under the FITS[1] format. The benefit of this format is the flexibility to add several image extensions.

3.2 Missing data processing

SPICAM and SPICAV observations can have missing packets due to the communication troubles between the satellite and the earth ground segment. The presence of missing packets in an observation causes a wrong total number of records (or spectra). Two spectra can be consecutive but are in fact separated by a certain gap time corresponding to missing data. This process purpose is to inject empty values to retrieve the correct number of records.

The criterion to look for gaps is the record time. New lines, corresponding to the detected missing records, are injected with NaN[2] values in the data array, for all the spectral points in the missing packet.

4 Correction process description

[1] *FITS: Flexible Image Transport System*
[2] *NaN: Not a Number, data type representing an undefined value, IEEE 754 standard*

4.1 Data overlapping correction

4.1.1 *Correction for SPICAM IR:*

All measurement data (Data and System monitor fields) originate from the output of controller 12 bit ADC (Analog-to-digital converter). The ADC operates in +/- 5V full-scale bipolar mode and its output is twos-complement binary code:

Value	Binary code
+2047	0111 11111111b
…	
+1	0000 00000001b
0	0000 00000000b
-1	1111 11111111b
…	
-2048	1000 00000000b

Table 4-1 : Correspondance between ADU and Binary code

The ADC data obtained in channels of photodetectors are processed afterwards. The following integer operations are performed:
- A sum of N ADC measurements of the signal with AOTF on is accumulated,
- Another sum of N ADC measurements of the signal with AOTF off is accumulated,
- Difference between these two sums is calculated,
- The difference is normalized (divided by N),
- 12 LSBs of the result is the data point.

Addition and division operations compensate each other in the sense that they do not change output numbers range compared to the input 12bits range. But subtraction is not compensated and doubles the output range – in fact data points are 13bit signed integer values. Since only 12LSbits are transmitted the sign bit of data points is truncated.
In result when the signal begins to grow and reaches 2048, it falls to -2048 and continues to grow again in negative units. This must be taken into account when treating the device data.

The first correction of the data overlapping is computed with the following formula:

$$S_i(f) = 4096 + S_i(f) \quad if\ S_i(f) < -1000$$

Where $S_i(f)$ is a signal of ***i*** channel at frequency *f* in ADU.

4.1.2 Correction for SPICAV IR:

The same problem exists for the SPICAV IR channel. During observations of solar occultation and nadir observations with small SZA (<40) the signal in ADU of SW channel can exceed values of 5000 and even 7000. The data is cut off to 12 bit digital signed word. So if the value is:

- *A=5000*, it will be A_{sp}*=904*,
- *B=3500*, it will be B_{sp}*=-596*.

The conversion of data to real digital value has to be done before the calibration of IR channel. If a full spectrum was recorded the correction is computed with following formula:

$S_i(f) = 4096 + S_i(f) \quad if\ S_i(f) < -100$ and TIME<3ms and *f*>140 MHz (SW channel)

$$S_i(f_{i+1}) = 4096 + S_i(f_{i+1}) \quad if\ (S_i(f_i) - (S_i(f_{i+1})) > 3500$$

Where

- $S_i(f)$ is a signal of ***i*** channel at frequency *f* in ADU
- TIME is the AOTF integration period
- *f* is the radio frequency in MHz.

The algorithm is more difficult for the DOTS set. The set of DOTS can be found in the *commands-configs-FM2b_XXXX_xxx.xls* file. The sets have been fixed before the flights and can't be changed. 4 spectral points of the SW channel are used in the DOTS set. Flight configurations 4 and 7 are used all the time with these 4 points. The new special algorithm for these DOTS has been developed and implemented for TIME<3 msec. The algorithm takes into account relative variations of solar intensity and detector's sensitivity between SW points separates up to 100 nm. It is not worked for any other sets of SW DOTS, but due to only this set was regularly used we have not pay attention to the more common algorithm.

4.2 Dark Current correction

4.2.1 Correction for SPICAM IR

The measurements of the AOTF spectrometer are based on digital synchronous detection, and for each measurement the dark signal is subtracted from the useful signal. Still, some background signal may propagate owing to synchronized optical or electrical interference. The synchronized RF interference from the AOTF driver was significant for the Mars version of the instrument, forming a characteristic pattern in function of wavelength [3, 4].

This kind of interference depends on radio frequency (RF) and power, and forms a characteristic pattern as a function of wavelength. This pattern, well characterized on the ground, has changed after the launch with a minimum, which appeared around 1.35 μm. Also, we have noticed slight modifications of the background as a function of the observation mode (Nadir, Limb, etc.), due, most likely to the modification of the thermal regime. A special effort has been dedicated to characterize the background behavior in flight, as a function of particular observation modes, and including the dependence on temperature and other parameters. To support this study, the IR spectrometer is maintained on during most of operations when no significant signal in the IR is expected.

As soon as the background signal is determined, the correction procedure is trivial and consists of subtraction of the averaged smoothened background signal ("Dark Current" (DC)) from each measured spectrum. The radiation coming from the planet can be presented as:

$$S = M - D$$

Where

- M is a measured signal
- S is a source signal
- D is a dark current

The DC has a temperature and RF dependence. Depending on the command set, there are several formulations to estimate the dark current: constant, linear and quadratic polynomial approximation, as shown in the following table:

Case	DAC	GAIN	TIME [ms]	Dark Current
1	1744	8.25	5.6	$D_g(f)=a_d(f)\times T^2+b_d(f)\times T+c(f)$
2	1504	3.0	5.6	$D_g(f)=a_d(f)\times T+b_d(f)$
3	1744	3.0	2.8	$D_g(f)=a_d(f)$

Table 4-2 : Formulations of the Dark Current estimation

Where

- TIME is the AOTF integration period.
- GAIN is the amplifiers gain factor.
- DAC is the AOTF RF power control
- D_g is the dark signal in ADU/gain factor
- T is the temperature of detectors in Volts
- f is the radio frequency in MHz.

The coefficients a, b and c are given for sequence of frequencies from 84 to 147 MHz with step 0.5 MHz for cases 1 and 2 and step 0.192 MHz for case 3. The coefficients are different for detectors 0 and 1.

The first case (DAC=1744, GAIN = 8.25, TIME = 5.6 ms) is a main mode of nadir observation. Finally, the DC for each frequency could be obtained as

$$S(f) = M(f) - D_g(f) \times GAIN$$

4.2.2 Correction for SPICAV IR:

For SPICAV the DC is much weaker compared to SPICAM but still it has to be taken into account during the data treatment especially for low signal. The cooling of the detectors substantially decreases the DC and noise and it is preferentially used in flight [5].

A special effort has been dedicated to characterize the background behaviour in flight, as a function of particular observation modes, detector's temperature, integration time and gain. To support this study, the IR spectrometer was powered in the most practical observation regimes during several orbits when no significant signal in the IR was expected (e.g., while SPICAV UV observes in stellar occultation modes, away from the planet's disk).

1) The DC was measured for 3 main commands and Peltier on and off:
   - TIME=2.8 ms, GAIN=8
   - TIME=89.6 ms, GAIN=8
   - TIME=89.6 ms, GAIN=16.
2) DC is significantly different for the two polarizations (Channels 0 and 1) owing to different electrical interference.
3) the DC is lower in the SW channel, while in the LW channel it is more variable.
4) The DC and its variations are especially important for the observations of weak signals on the nightside.
5) For the dayside observations the DC can be considered insignificant both for LW and SW channels. On the other hand, a good knowledge of the background for both detectors is a must for polarization studies on the dayside, when the difference of two polarizations can be less than 1%.

As soon as the background signal is determined for each TIME and GAIN, the correction procedure is trivial and consists of subtraction of the averaged smoothened background signal from each measured spectrum:

$$S = M - D$$

4.3 Wavelength calibration

The tuning curve of an AOTF can be described as $\lambda \sim \frac{a}{f}$. The dispersion of the AOTF crystal changes with temperature, and the wavelength assignment of the AOTF spectrometer is expected to change with the drift of the crystal temperature owing to internal heat dissipation or environmental conditions (relative wavelength shift is ~$1.6 \cdot 10^{-2}$ nm K^{-1}). The AOTF unit is equipped with a sensitive temperature sensor in the proximity of the crystal.

4.3.1 Calibration for SPICAM IR:

We treat temperature as a quadratic perturbation to both coefficients *a* and *b*:

$$a, b = x + yt + z\,t^2$$

Where coefficients *x*, *y*, z are listed in the *Table 4-3*. The dispersion curve parameterized as:

$\lambda = a/f + qf^2 + b$ *for channel 0*

$\lambda = a/f + b,$ *for channel 1*

Where

- $q = -6.53\ 10^{-11}$
- λ is the wavelength expressed in nanometers
- *f* is the frequency in kHz
- *t* is the temperature measured by the sensor in degrees Celsius.

The accuracy of this calibration is better than ±0.2-0.3 nm within the range of 1100-1600 nm.

	X	*y*	*z*
Channel 0			
a	$1.367\ 10^{8}$	0	0
b	74.43	0.0285	10^{-4}
Channel 1			
a	$1.3690971\ 10^{8}$	2464.6217	–3.6228649
b	71.220396	$4.4824233\ 10^{-3}$	$-5.4920304\ 10^{-6}$

Table 4-3 : Fit coefficients for the wavelengths calibration curve.

And in the units of wavenumber it can be approximated as:

$$\nu = af^2 + bf + c, \qquad (1)$$

Where:

- ν is the wavenumber expressed in cm^{-1}
- *f* is the frequency in kHz.

4.3.2 Calibration for SPICAV IR:

The typical temperature of SPICAV in-flight is around –10°C varying from –21° to –4°C. The calibration with solar lines for AOTF temperature of –10°C was accepted as a reference. The coefficients *a, b,* c of the equation for the in-flight calibration are listed in the Table 4.3.2 for both channels and detectors. The dispersion is slightly different for two output polarizations of the AOTF

(channels 0 and 1). The accuracy of this calibration is better than ±0.3 nm and ±0.5 nm within the LW and SW ranges respectively, including the uncertainty due to the temperature shift.

	a	*b*	*c*
Short wavelength channel (SW)			
Channel 0	-4.9405101e-008	7.6969006e-002	-2.9822051e+002
Channel 1	-5.0454785e-008	7.7358519e-002	-3.3244465e+002
Long wavelength channel (LW)			
Channel 0	-3.3865473e-008	7.2595705e-002	-2.0449838e+000
Channel 1	-3.5371703e-008	7.2919764e-002	-1.9140569e+001

Table 4-4 : Polynomial coefficients for the wavelengths calibration curve (Eq. 1)

4.4 Correlation of geometry and data points

4.4.1 Correlation for SPICAM IR:

SPICAM IR operates as point spectrometer and measures intensity at each wavelength sequentially. The sequence of AOTF frequencies (further converted into wavelengths) contains several blocks (usually 2 or 3) with 664 spectral points (332 pts for each detector) in each block. The time of the beginning of spectrum record (T_{sp}) is presented before each spectrum.

In course of measurement cycle the buffer is getting filled until one of the following conditions is met: 1)accumulated data fit the capacity of data blocks (in this case measurement is paused until data transfer), 2)measurement cycle is over, 3) command is received.

The geometry data also relates to defined time. So the correspondence between data and geometry is defined through the time of measurements. In geo data the first time corresponds to the beginning of first spectrum and time step corresponds to time of one block record:

TIME, ms	Block size, sec
2.8	1
5.6	2
11.2	4

.

The corresponding geometry can be found for each spectral point as

N_{bl}=fix(n/332) (round to zero) – to find which block corresponds to this spectral point

$T_{obs}=T_{sp}+N_{bl}*T_{bl}+(n-N_{bl}*332)*TIME*10^{-3}$; - to find exact time of the point

Where T_{obs} is the time corresponding of the spectral point

n is a number of spectral point

TIME, ms is the AOTF integration period

N_{bl} – number of block in the spectrum (from 0)

T_{bl} is the time of block record and transfer (2 sec for TIME=5.6 ms)

Example:

Typical solar occultation spectrum consists of 664 spectral points: 2 blocks and 4 sec totally. One spectral point takes 5.6 ms. T_{bl}=2 sec.

The 1.43 µm H_2O band is located between 300 and 600 spectral points. Assume T_{sp}=0 sec

$T_{obs}(300)=0+0*2$ sec$+(300-0*332)*5.6\ 10^{-3}=1.68$ sec

$T_{obs}(600)=0+1*2$ sec$+(600-1*332)*5.6\ 10^{-3}=3.5$ sec

When the geometry for these times can be calculated from the interpolation with times in geo data and the geometry for the H_2O band should be averaged between these times.

The exact time of spectral point is especially important for limb measurements and solar occultations when the altitude of target point in the atmosphere changes with time. Users should take it into account when trying to find out the height corresponding to each spectral region.

4.4.2 Correlation for SPICAV IR:

The same reasoning should be taking into account for SPICAV IR except the geometry data are presented with step corresponding of the beginning of each spectrum and :

TIME, ms	Block size, sec
2.8	1
5.6	2
11.2	4
22.4	8
44.8	15
89.2	30

4.5 Radiometric calibration

4.5.1 SPICAM IR

The accuracy of ground data on the absolute sensitivity of SPICAM IR was low, and the absolute calibration of SPICAM IR in flight was repeated by comparing with spectra measured by OMEGA mapping spectrometer on Mars Express [*Bibring et al.*, 2004]. One OMEGA pixel is only 4.1 arc min against 1° FOV of SPICAM, in turn spectral sampling of OMEGA is 13 nm in the spectral range of interest against 0.6 nm for SPICAM. We compared SPICAM spectra convolved to OMEGA spectral resolution with OMEGA spectra integrated over the SPICAM FOV for a few orbits (30, 68, 278, 103, 368) with relatively homogenous surface albedo. The chosen orbits correspond to different parameters of SPICAM operation. After that, the calibration coefficients for each spectral point have been calculated as follows:

$$k[\mathrm{ADU}/(\mathrm{W/m^2/\mu m/sr})] = \mathrm{SPICAM[ADU]/GAIN} \,/\, \mathrm{OMEGA\ [W/m^2/\mu m/sr]} \qquad (1)$$

The reported accuracy of OMEGA calibrations is superior to 15%. SPICAM noise-equivalent brightness (NEB) for a sampling of 5.6 ms and reaches in the best case the value of 0.1 W/m^2/μm/sr that is better than the value, estimated from laboratory measurements using a calibrated tungsten lamp and sun atmospheric measurements [*Korablev et al.*, 2002].

Special efforts have been taken to provide additional calibrations of the polarization properties of the instrument in flight. To cross-calibrate the sensitivity of the two detectors we used opposition observations when phase angle (or solar zenith angle for nadir observations) equals zero, because in such case the polarization degree equals zero for symmetry reasons. This situation occurs every time when the orbital plane intersects the sun. The measurements have been performed in orbit 168 with the spectral coverage of 1050-1650 nm. The measured ratio of signals in two polarization channels (detector 0/detector 1) has been used to correct the radiance calibration for the second detector.
Resulting radiance has been obtained as:

$$R = \frac{\mathrm{S}}{\mathrm{GAIN}\ k\ k_{pol}}$$

k_{pol} is the polarization correction curve.

4.5.2 Correcting long term trend in SPICAM IR

In 2025, we revisited the calibration to take into the aging of the detectors. For the channel 0, we both compared SPICAM with OMEGA on a larger sample of hundreds of joint nadirs up to orbit 9000 with a similar method than the one described in the previous paragraph. And we also investigated the evolution of the average signal from the sun observed by SPICAM during solar occultations. We found comparable trends from comparing SPICAM/OMEGA and from solar observations with a decrease of roughly 20% of the signal during the mission.

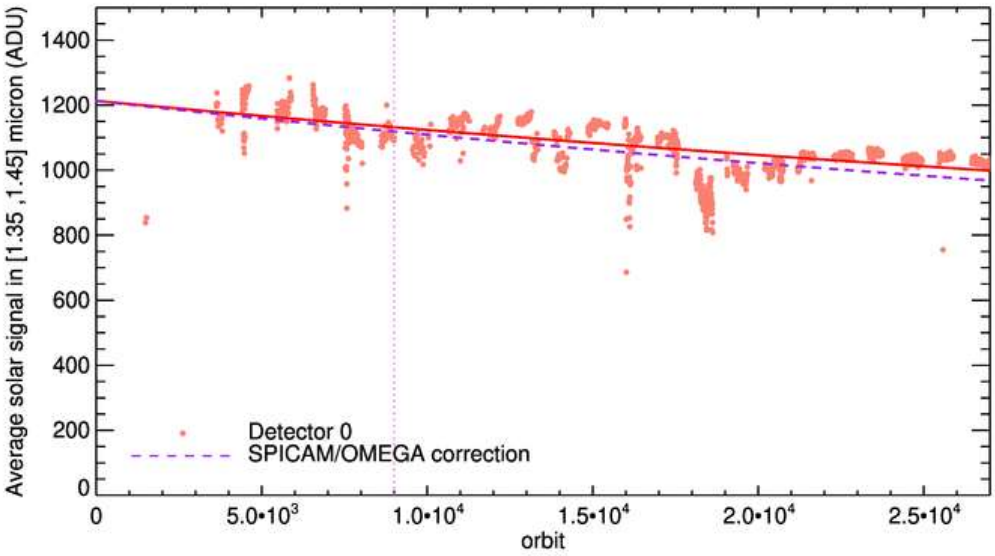

For the channel 1, we extracted directly the trend from the solar observation.

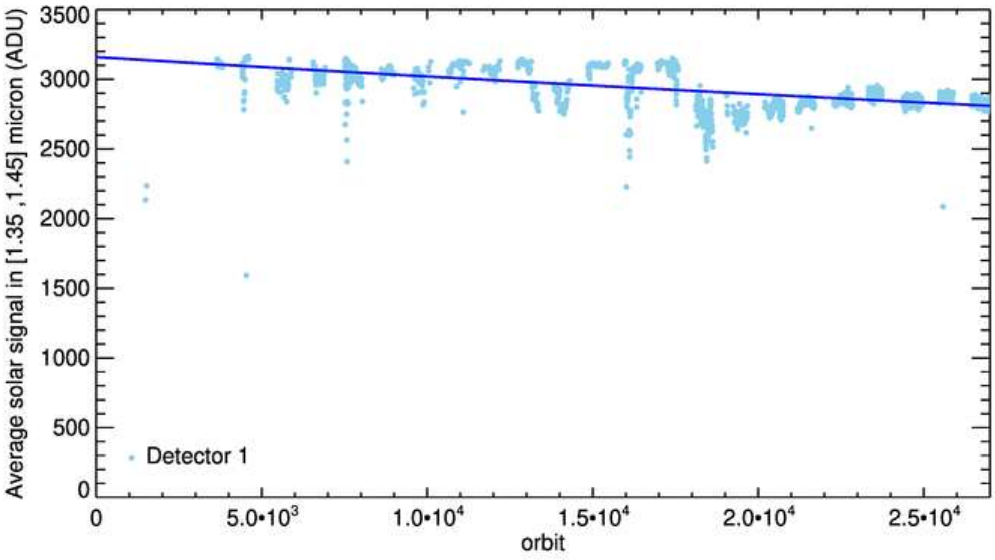

To correct the signal from the aging trends observed in solar observations, we updated the calibration coefficients *k'* using a linear model:
k'[ADU/(W/m^2/µm/sr)] = k[ADU/(W/m^2/µm/sr)] * (1 + coeff *orbit number)

Channel	coeff
0	7.9539712e-06
1	4.6051532e-06

4.5.3 SPICAV IR

The sensitivity calibration in the laboratory was to a band-shape filament tungsten lamp. The instrument response has been recorded for different integration times and gain values. The curves demonstrate also the sensitivity of the instrumental response to the cooling of the detectors, in particular near their long-wavelength cutoff (short frequencies), owing to photoelectric threshold.
The nominal temperature of the calibration lamp during the laboratory measurements was 2500 K. Approximated by the Planck function its spectral curve allows to estimate the sensitivity in absolute units (W/m^2/μm/ster). The laboratory measurements have been performed for a subset of integration times (T_M = 2.8, 5.6, 11.2, 22.4 ms), and gain values (G=1…16), but not for sensitive modes with high gains and long integration times aimed for nightside observations (T_M = 44.8 and 89.6 ms). The absolute dayside calibration was rectified in flight using Venus albedo data (Moroz, 1981).

We checked the absolute calibration of SPICAV IR in flight against the spectra measured by VIRTIS-M mapping spectrometer on Venus-Express (Drossart et al., 2007a; Cardesín et al., 2010). One VIRTIS-M pixel is only 0.25 mrad (0.86 arc min) against 2° FOV of SPICAV IR, in turn spectral sampling of VIRTIS-M is 13-17 nm in the near-IR against 0.9 nm for SPICAV. We compared SPICAV spectra convolved to VIRTIS spectral resolution with VIRTIS-M spectra integrated over the SPICAV IR FOV for a few orbits with relatively homogenous cloud albedo. The chosen orbit corresponds to typical day-side (T_M =2.8 ms and G=2) command of SPICAV IR used as the dayside reference. Again, we noticed the modification of the sensitivity in the LW channel after the launch. It has further degraded (by a factor of ~0.6) in the vicinity of 1300-1500 nm depletion, and remained stable for the whole duration of flight. We used VIRTIS data to correct the 1300-1500 nm range calibration.
The absolute calibration obtained for the reference observation command can be scaled to all other combination of T_M and G using the values from Table.

Table. Overall amplification factor F of SPICAV IR in function of measurement time (T_M) and preamplifier gain (G) parameters normalized to basic calibration mode (T_M =2.8 ms and G=2).

T_M\G	1	2	4	8	16	32	64	128
1.4	0.227337	0.39096	n/a	n/a	n/a	n/a	n/a	n/a
2.8	0.563713	1	2.31461	3.60981	n/a	n/a	n/a	n/a
5.6	1.23647	2.21808	3.41675	8.09193	17.4423	n/a	n/a	n/a
11.2	2.58197	4.65424	7.26966	17.0562	36.6292	75.7753	n/a	n/a
22.4	5.27298	9.52656	14.9755	34.9847	75.0031	155.04	315.113	n/a
44.8	12.4231	23.8269	43.5761	70.8417	151.751	313.569	637.205	1284.48
89.6	26.7234	52.4275	100.777	185.244	305.246	630.627	1281.39	2582.91
179.2	55.3241	109.629	215.18	414.049	762.856	1264.74	2569.76	5179.78

We estimate the accuracy of the resulting absolute calibration as within 20% for all tested combinations of and G.

Because of birefringent properties of TeO_2 crystal, the AOTF separates the incoming beam into two diffracted beams, which illuminate two detectors. The two beams are fully linearly polarized, with orthogonal directions. We have measured the polarization capabilities in the laboratory using the SPICAV IR spare flight model. The AOTF crystal inside SPICAV IR is oriented with respect to the spacecraft coordinates X, Y, Z, with the polarization axes coinciding with X and Z. Nadir coincides with the Y direction. The nominal attitude of the spacecraft is “solar optimized”, which means that the sun is kept always in the XY plane, and the solar panels are rotated around Z to maintain them perpendicular to the sun. Special efforts have been taken to provide additional calibrations of the polarization properties of the instrument in flight. To cross-calibrate the sensitivity of the two detectors we used opposition observations when phase angle (or solar zenith angle for nadir observations) equals zero, because in such case the polarization degree equals zero for symmetry reasons. This situation occurs every time when the orbital plane intersects the sun. The measurements have been performed for several orbits 464-01, 1472 and others with the most complete coverage of

the full spectral range 690-1640 nm. The measured ratio of signals in two polarization channels (detector 0/detector 1) has been used to correct the laboratory measurements.

Resulting radiance for two detectors has been obtained as:

$$K = k\,F\,\mathrm{GAINBOOST}$$

$$R = \frac{\mathrm{S}}{K\,k_{virtis}k_{pol}}$$

Where k is the calibration coefficient obtained in laboratory,
F is the correction coefficient from the table for gain of the integrating amplifier (GAIN) and T_m
GAINBOOST is the gain (1 or 4)
k_{virtis} is the correction curve for VIRTIS data
k_{pol} is the polarization correction curve.